Small-Angle X-ray Scattering (SAXS) Studies of Sulfonated Polystyrene Ionomers. 1. Anomalous SAXS

Benjamin Chu* and Dan Q. Wu†

Chemistry Department, State University of New York at Stony Brook, Long Island, New York 11794-3400

Robert D. Lundberg

Corporate Research Science Laboratory, Exxon Research and Engineering Company, Clinton Township, Route 22 East, Annandale, New Jersey 08801

William J. MacKnight

Department of Polymer Science and Engineering, University of Massachusetts, Amherst, Massachusetts 01003

Received June 1, 1992; Revised Manuscript Received October 13, 1992

ABSTRACT: Morphological studies of sulfonated polystyrenes by using small-angle X-ray scattering (SAXS) and anomalous SAXS (ASAXS) are presented. ASAXS was used to study a model ionomer system: zinc salts of sulfonated polystyrene (SPS). The results showed the presence of local clustering, as well as long-range inhomogeneities of ions. The observed morphology could be attributed only to the metal ionic structures, as can be proven by means of ASAXS. However, with the SAXS patterns by SPS being much stronger than those of polystyrene or SPS in acid form, the excess SAXS patterns of the metal ions can be measured with greater precision by SAXS than by ASAXS.

I. Introduction

The morphology of ionomers has been studied extensively by many workers,[1] primarily using small-angle X-ray scattering (SAXS)[2-11] and small-angle neutron scattering.[11-14] In the past few years, Cooper and his co-workers made direct observation of ionic aggregates in sulfonated polystyrene ionomers[15] and observed an aggregate size of approximately 3 nm in Ni^{2+} and Zn^{2+} neutralized sulfonated polystyrenes (SPS). Register et al. used extended X-ray absorption fine structure (EXAFS) spectroscopy and found the local coordination structure about the Mn^{2+} cation to be unaltered by ionic aggregation.[16] More importantly, Ding et al.[17a] and Register and Cooper[17b] used anomalous small-angle X-ray scattering (ASAXS) to study nickel-neutralized ionomers. The SAXS profiles were generally acquired at 50 and 5 eV below the Ni^{2+} K-edge. The difference SAXS profile formed from two different X-ray energies was superimposable with the single-energy SAXS pattern after appropriate scaling. Their observations proved that both the ionomer peak and the upturn near zero angle were due to an inhomogeneous distribution of ionic repeat units throughout the material and not to precipitated neutralizing agent or microvoids. Register and Cooper extended the ASAXS studies to a nickel-neutralized poly(ethylene-*co*-methacrylic acid) ionomer,[18] which was consistent with a three-phase morphological model, incorporating lamellar crystallites, interlamellar amorphous polymeric material, and ionic aggregates residing within the amorphous layers. In addition, Cooper and co-workers also studied sulfonated polyurethane[19,20] and carboxy-telechelic polystyrene[21] ionomers.

With the availability of synchrotron radiation at the National Synchrotron Light Source (NSLS), we have also started a program for ionomer studies using a modified Kratky block collimator[22] and an X-ray photodiode array detector.[23] We note that precise SAXS profiles over a very broad q range[24] can be achieved by using synchrotron radiation. The low q range accessible by the modified Kratky block collimator permitted us to investigate more closely the long-range inhomogeneities in sulfonated polystyrene ionomers.[25] We have also made a preliminary report on SAXS of poly(ethylene–methacrylic acid) lead and lead sulfide ionomers.[26]

In this paper we report ASAXS and SAXS profiles of ZnSPS starting with a very narrow molecular distribution in the original neutral polystyrene sample. In a companion paper, we perform a detailed correlation function analysis of our SAXS profiles and compare the results with interparticle and intraparticle interference models. The purpose of the present investigation can be summarized as follows.

We want to determine the energy-dependent atomic scattering factor $f(E)$ experimentally. After having carefully established the K-edge of Zn, SAXS experiments at selected energies are carried out. The difference SAXS profiles, after corrections for instrumental effects and fluorescence, etc., are compared with the SAXS profile measured at X-ray energies much lower than that at the K-absorption edge. The SAXS data, including the difference SAXS profiles from ASAXS, are used to investigate the nature of the small-angle upturn and the structure of the ionic peak. As Register and Cooper[17] have already excluded the possibility of precipitated neutralizing agent or microvoids in their ASAXS of nickel-neutralized sulfonated polystyrene ionomers as a reason for the small-angle upturn, our main task here is trying to experimentally measure a SAXS profile from very near the small-angle limit of SAXS to the scattering vector (q) range where the scattered intensity has fallen to near zero intensity.

II. Theoretical Background for ASAXS

In ASAXS, the SAXS profiles are measured at different selected X-ray energies from near an absorption edge to some lower X-ray energies away from the absorption edge

* Author to whom correspondence should be addressed.
† Present address: Polymer Products Department, Du Pont Experimental Station, Wilmington, DE 19880-0269.

0024-9297/93/2226-0994$04.00/0

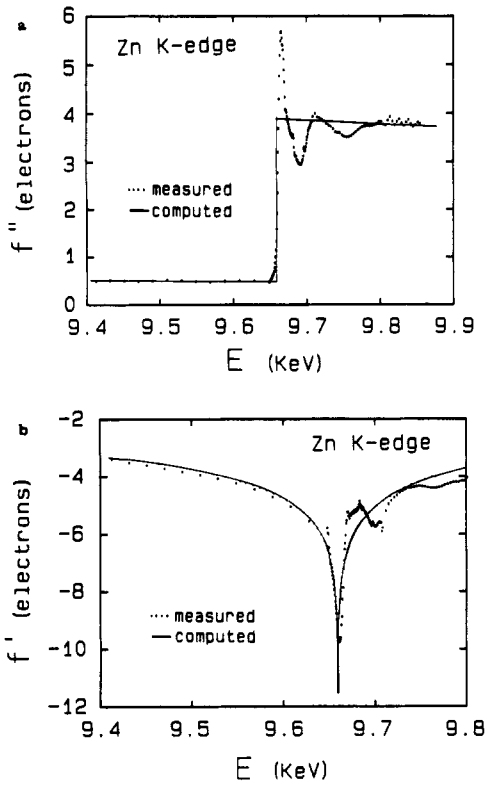

Figure 1. (a) Plot of f'' versus E. The computed values can be found in ref 28. (b) Plot of f' versus E by means of eq 3. The small dots on the computed curve are due to the discrete nature in the computation using eq 3.

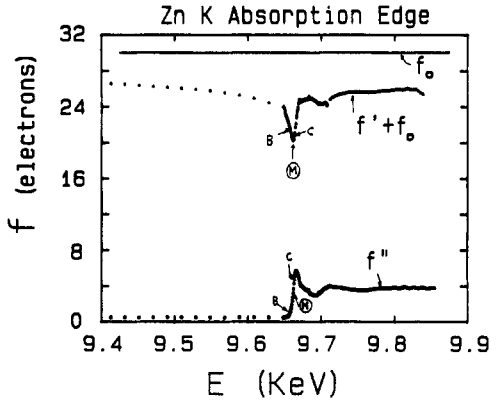

Figure 2. Plot of $f' + f_0$ and f'' as a function of E. M (=9661.6 eV) denotes the Zn K absorption edge. B (=9660 eV) and C (=9663 eV) are two of the selected energies used in the ASAXS experiment. The value 9663 eV has an X-ray energy slightly above the Zn K-edge, while 9660 eV has an X-ray energy slightly below the Zn K-edge.

of an element, such as the K-edge of Zn. The procedure is summarized as follows.

For a molecular system, the scattered intensity, $I(q)$, is expressed by

$$I(q)/I_e = F(q)\,F^*(q) = \sum_i \sum_j f_i f_j e^{-iq\cdot(\mathbf{r}_i - \mathbf{r}_j)} \qquad (1)$$

where I_e is the intensity scattered by a single electron, $\mathbf{r}_i$ is the position vector of object i, $q = (4\pi/\lambda)\sin(\theta/2)$, with λ and θ being the X-ray wavelength and the scattering angle, respectively, and f_i is the atomic scattering (form) factor of object i.

$$f(q,E) = f_0(q) + f'(q,E) + if''(q,E) \qquad (2)$$

where E ($=hc/\lambda$) is the energy of incident X-ray, with h and c being the Planck constant and the speed of light, respectively, f_0 is equal to the atomic number Z and is independent of energy, and f' and f'' are energy dependent and are known as the anomalous scattering factors. f' and f'' are relatively small in magnitude when compared with f_0, except for those X-ray energies near the atomic absorption edges where both f' and f'' show drastic changes.

Table I
f' and f'' at Selected Energies for ZnSPS

sample designation	f' (electrons)	f'' (electrons)	E (eV)	λ (Å)
A	−3	0.499	9281.1	1.3358
A′	−3.5	0.500	9432.2	1.3144
B′	−5.8	0.49	9648.3	1.2850
B	−9.44	1.91	9659.8	1.2835
M	−9.76	3.2	9661.6	1.2832
C	−9.67	4.3	9662.8	1.2831

In the anomalous small-angle X-ray scattering (ASAXS) technique, the universal features of f' and f'' (drastic energy dependence) at an atomic absorption edge of a selected element (normally a metal; in our case, the K-edge of Zn) are utilized in order to take advantage of the varying scattering power of the selected element with X-ray energy.

The imaginary part of the anomalous scattering factor, f'', is proportional to the absorption coefficient μ and is related to f' through the Kramers–Kronig dispersion relation

$$f'(\omega) = \frac{2}{\pi}\int_0^\infty [\omega' f''(\omega')/(\omega' - \omega^2)]\,d\omega' = \frac{2}{\pi}\int_0^\infty [E' f''(E')/(E^2 - E'^2)]\,dE \qquad (3)$$

In eq 3, $E^2 - E'^2 = (E + E')(E - E')$. Therefore, there is an irregular point at $E - E'$. Experimentally, a ΔE of ~0.2 eV was achieved. We used $E - E'$ ~0.05 eV and an integration limit corresponding to λ = 0.1–5 Å with a Zn (K-edge) having an X-ray energy of 9661.6 eV.

III. Experimental Methods

Materials. Zinc salts of sulfonated polystyrene have M_w = 1.15 × 10⁵, M_w/M_n = 1.04, ~4.5 (and lower) mol % of sulfur, 100% neutralized. The ionomer samples of the salts were compression-molded to films (~1 mm thick) at 230 °C (~2 min) at 29 tons of pressure/~4 cm² of polymer film cross section.

Beamline Optics. The SAXS at X3A2 SUNY beamline has been described elsewhere.[22,27] The monochromator has a double flat crystal with a fixed-exit geometry and can be tuned rapidly to select an energy without appreciable change in the incident beam direction exiting from the double monochromator. For ASAXS experiments, the gold-coated bent torroidal quartz mirror (60 cm long and 6 cm radius) was removed. The reduction in flux was compensated by the convenience in energy selection. Furthermore, an unfocused incident beam has a smaller divergence than a focused beam (at ~ 10 M away from the mirror) because of the nature of synchrotron radiation. Thus, without a focusing mirror, a smaller scattering angle can be achieved more conveniently using the Kratky block collimator. With a beam width of 0.2 mm, $q \approx 0.03$ nm⁻¹ has been achieved.[24] A Braun linear position-sensitive detector was used to measure the SAXS profile.

IV. Results and Discussion

Figure 1a shows a plot of f'' as a function of E. With eq 3, f' was computed as shown in Figure 1b. The purpose of repeating the experiment on what is already known in the literature is to calibrate our SAXS instrument so that we could come as close to the Zn K-edge as possible, in order to achieve the maximum signal-to-noise ratio in the difference ASAXS profile. Figure 2 shows a plot $f' + f_0$ and f'' versus E in which the selected energies (B and C)

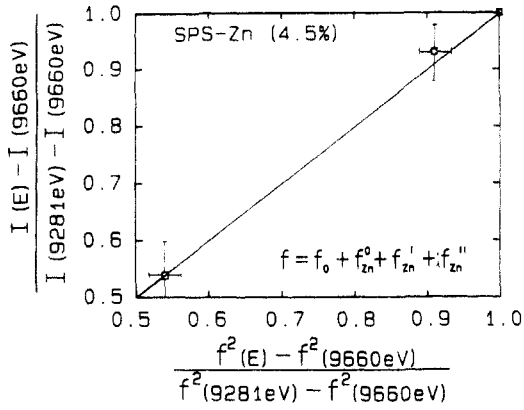

Figure 3. Plot of $[I(E) - I(9660\text{ eV})]/[I(9281\text{ eV}) - I(9660\text{ eV})]$ versus $[f^2(E) - f^2(9660\text{ eV})]/[f^2(9281\text{ eV}) - f^2(9660\text{ eV})]$ for ZnSPS at a fixed q.

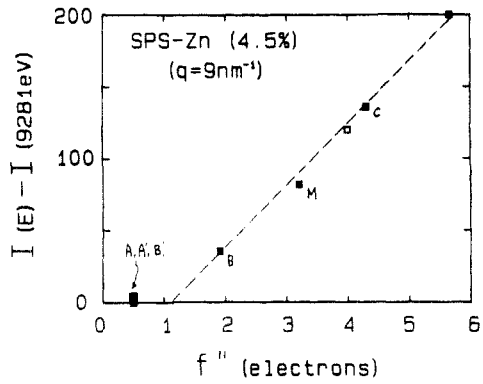

Figure 4. Plot of $I(E) - I(9281\text{ eV})$ versus f''. The letters denote sample designations listed in Table I.

for the ASAXS experiment, as well as the Zn K-edge (M) are shown. From Figure 2, we can also compute the percent change in scattering power, because we have come very close to the Zn K-edge as listed typically in Table I. To get the maximum effect, we want a minimum $|f''|$ and a maximum $|f'|$, but at E below the Zn K-edge in order to minimize other effects, such as fluorescence.

For the scattering curves, $I(q)$ represents the scattered intensity which has been corrected for incident X-ray intensity fluctuations, absorption, detector linearity, dark count, sample thickness, detector alignment, and stray X-ray background.

From eq 1, $I(q,E) \propto |f|^2$ where $f = f_{0,Zn} + f'_{Zn} + if''_{Zn} + f_0$, with f_0 denoting the energy-independent atomic scattering factor of all the other elements in the system. For the difference scattered intensity, $\Delta I(E_2 - E_1)$, measured at two different selected energies, the normalized value should be proportional to the normalized $f^2(E_2) - f^2(E_1)$:

$$\frac{I(E) - I(E{=}\mathrm{B})}{I(E{=}\mathrm{A}) - I(E{=}\mathrm{B})} = \text{constant}\frac{f^2(E) - f^2(E{=}\mathrm{B})}{f^2(E{=}\mathrm{A}) - f^2(E{=}\mathrm{B})} \qquad (1')$$

since the structure factor has remained the same. Figure 3 shows such a plot.

In an ASAXS experiment, it is also necessary to take into account the undesirable effects, such as fluorescence, due to measurements of scattered intensities near the absorption edge. One empirical procedure for such corrections is to perform an experiment at a q value where the scattered (or diffracted) intensity has fallen down to a very low value and is a small fraction of the intensity due to other effects. Figure 4 shows a plot of $I(E) - I(9281\text{ eV})$ versus f'' measured at X-ray energies mostly listed in Table I. At A and B, the X-ray energies were sufficiently below the Zn K-edge. Therefore, no fluorescence was observed.

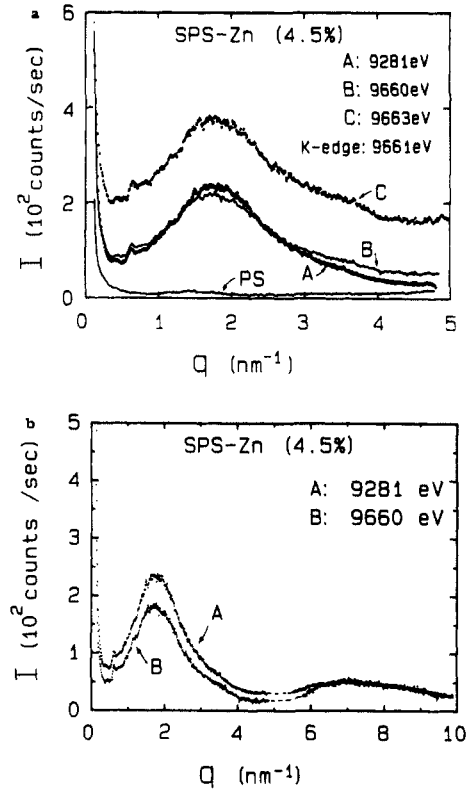

Figure 5. (a) Plot of measured apparent scattered intensity I^* as a function of q at different X-ray energies. The Zn K-edge is located at 9661.6 eV. A polystyrene curve measured at E = 9281 eV is also included for comparison. (b) Plot of scattered intensity after subtraction of fluorescence in curve B as a function of q. In order to achieve a proper correction, one has to perform the experiment at a q-value where the intensity contribution due to the ions is known to be very samll.

The excess intensity becomes noticeable as f'' begins to change, as revealed by Figures 1a and 3. In Figure 4, we have assumed that, at E = 9281 eV, only normal scattered intensity was observed. The $I(E) - I(9281\text{ eV})$ value also represents the excess intensity due to other effects. We shall also assume that fluorescence is independent of q. Figure 5a shows a plot of the measured apparent scattered intensity (after corrections), I, as a function of q using different X-ray energies. The much higher apparent scattered intensity for curve C with E at 9662.8 eV $\simeq$ 9663 eV is due to strong fluorescence at X-ray energies higher than the Zn K-edge. In order to correct for the fluorescence effect, we force curves A and B to overlap at q = 9 nm^{-1} as has been calibrated according to Figure 4. The forced overlap of the A,B curves at q = 9 nm^{-1} resulted in a lowering of curve B, as shown in Figure 5b. In the correction procedure for the fluorescence, we have assumed that there is *no* fluorescence for curve A at all values of q and that the fluorescence in curve B is independent of q. The difference of the two curves, i.e., curve A − curve B or $I(9281\text{ eV}) - I(9660\text{ eV})$, is shown in Figure 6a. We have also included another difference SAXS profile measured at E = 9648.3 eV (or sample designation B') and at E = 9659.8 eV (curve B). The lower difference curve in Figure 6a has an inferior signal-to-noise because the X-ray energy at 9648 eV is already fairly close to the Zn K-edge. The shapes of the two curves can be shown to be identical by taking the ratio of the two difference SAXS profiles, as shown in Figure 6b. Figure 6a represents the net SAXS profile of Zn ions. It is the straightforward method to determine the structure of Zn ions. However, if the SAXS profile from the polystyrene backbone is

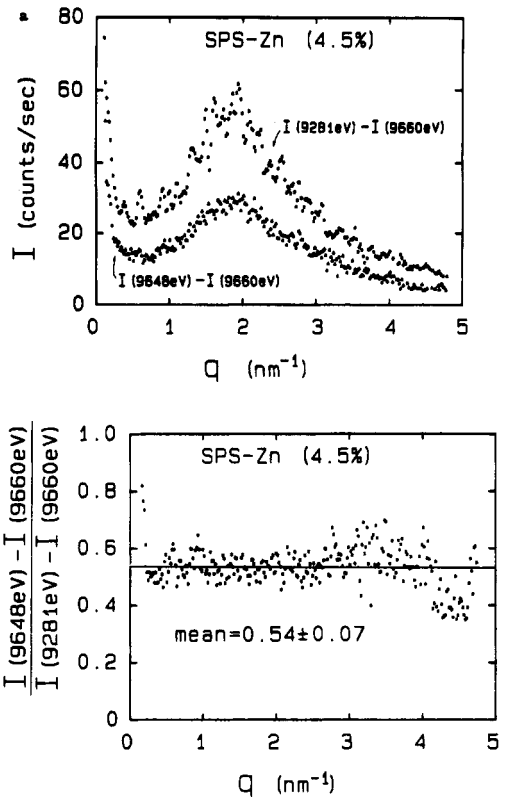

Figure 6. (a) Plots of two difference ASAXS profiles using three selected X-ray energies. (b) Plot of the ratio of difference ASAXS intensities as a function of q. The constant ratio illustrates that the shapes of the two difference ASAXS profiles are the same.

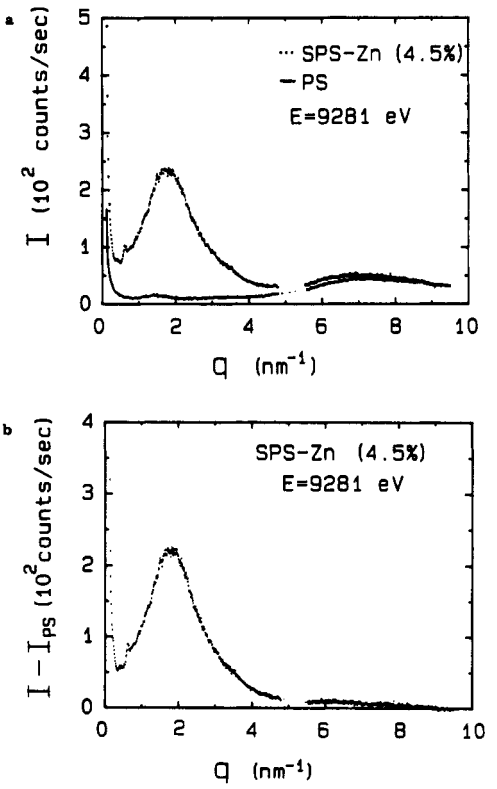

Figure 7. (a) Plots of SAXS profiles of SPS-Zn and PS at E = 9281 eV. The SAXS profiles coincide at $q > 8$ nm^{-1}. (b) Plot of SAXS profile due to zinc sulfonate at E = 9281 eV.

relatively weak, it may be possible to determine the excess SAXS from Zn by subtracting the SAXS profile of polystyrene (PS) from that of SPS-Zn.

SPS has an amorphous backbone. The presence of ionic aggregates should not alter the amorphous backbone

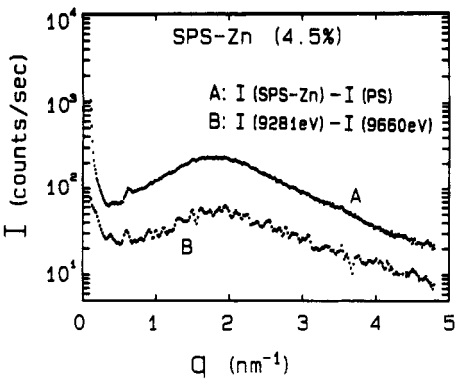

Figure 8. Comparison of difference SAXS profiles from [I(SPS-Zn) - I(PS)], curve A in Figure 8 (from Figure 7b), and [I(9281 eV) - I(9660 eV)], curve B in Figure 8 (from upper curve of Figure 6a).

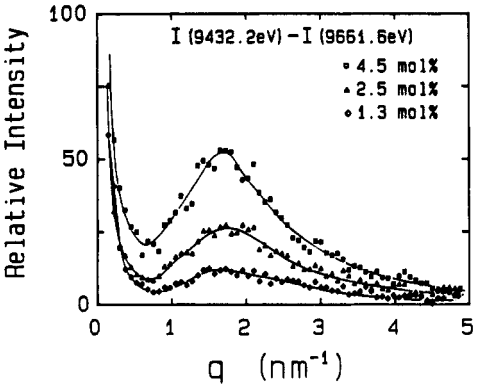

Figure 9. ASAXS difference scattering profiles of Zn ions in SPS-Zn containing, respectively, 4.5 (squares), 2.5 (triangles), and 1.3 mol % (diamonds) or sulfur. The curves were obtained by subtracting the SAXS profile at E = 9661.6 eV (after a fluorescence correction) from that at E = 9432.2 eV.

structure significantly in the SAXS range. In the absence of anomalous dispersion, f_0 is 30 for zinc, 16 for sulfur, 8 for oxygen, 6 for carbon, and 1 for hydrogen. The scattering from hydrogen is negligible, while the scattering from sulfur should be considered. If we take the sulfonic group, $-SO_3^-$, as a scattering entity, its averaged atomic scattering factor is $(16 + 3 \times 8)/4 = 10$. Therefore, the difference profile from I(SPS-Zn) - I(PS) should be a reasonable approximation to the zinc ion-related intensity.

Figure 7a shows the SAXS profiles of SPS-Zn and of PS measured at E = 9281 eV. The difference SAXS profile I(SPS-Zn) - I(PS) measured at E = 9281 eV is shown in Figure 7b. In the subtraction we have taken the SAXS intensity by zinc sulfonate to be zero at q = 9 nm^{-1}. A comparison of the difference SAXS profiles from Figure 7b and the upper curve of Figure 6a is shown in Figure 8. The shapes of the two curves remain identical. Thus, we have shown that we do not really need to use ASAXS to determine the SAXS profiles for Zn ions. The SAXS profiles for zinc sulfonate determined from the difference in the SAXS profiles of SPS-Zn and PS are comparable in shape and have better signal-to-noise ratios because of the much lower SAXS intensity from PS.

The SAXS profiles of Zn ions in SPS-Zn containing different mole percents of sulfonation, 1.3, 2.5, and 4.5 mol %, have been determined. Figure 9 shows ASAXS difference scattering profiles of Zn ions in SPS-Zn containing 4.5 (squares), 2.5 (triangles), and 1.3 mol % (diamonds) of sulfur. A closer comparison of the difference scattering patterns of SPS-Zn containing 4.5 (a), 2.5 (b) and 1.3 (c) mol % of sulfur which have been obtained by using ASAXS (triangles guided by a solid line) and by

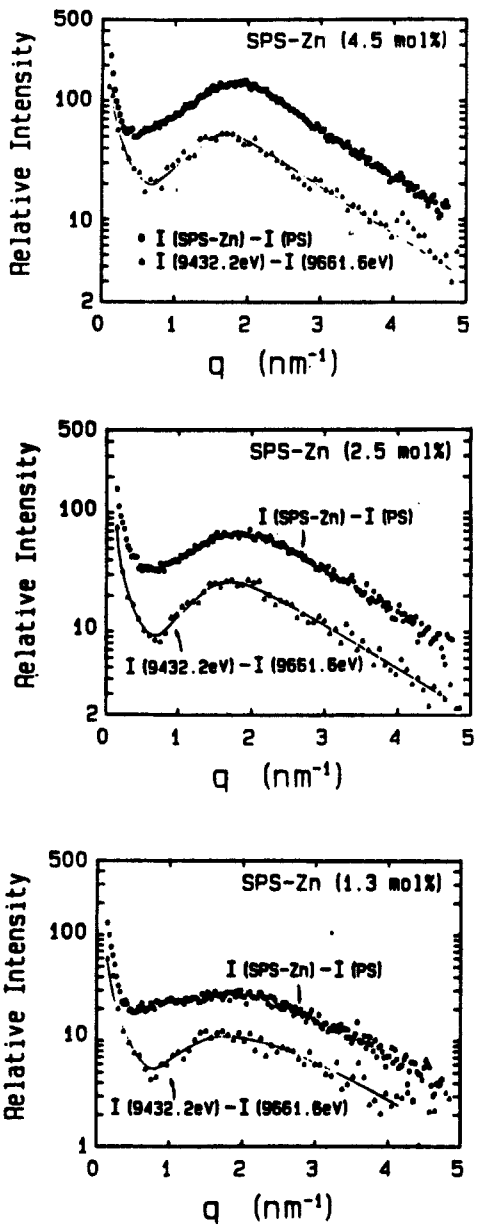

Figure 10. Comparisons between the ASAXS difference scattering profile (triangles with guided line) and the SAXS difference scattering profile for SPS-Zn containing 4.5, 2.5, and 1.3 mol %. Coincidence between the two curves was observed for $q > 2$ nm^{-1}. The difference, however, appeared at small scattering angles, e.g., $q > 0.8$ nm^{-1}.

using PS as background (squares) shows the following points.

(1) The ASAXS difference scattering profiles are always lower in magnitude than the corresponding SAXS difference scattering profiles.

(2) ASAXS nets only a fraction of scattered intensity, estimated by $2\Delta f'/f_0$, as the pure intensity from metal ions. In Figure 10, two curves show a good coincidence for $q > 2$ nm^{-1}. The ionic peak position in 4.5 mol % SPS-Zn (a) from ASAXS is located at a lower q value than that from the SAXS difference profile using PS as background. This set of results (a) is slightly different from the ASAXS difference curve in Figure 8. Therefore, for quantitative determinations, the ionic peak can be established more precisely by using the SAXS difference profile with PS as background. More importantly, the SAXS profile difference in the small q range, i.e., $q < 1$ nm^{-1}, is quite pronounced. The sharper upturn from ASAXS might be attributed to the sulfonate term in the SAXS procedure

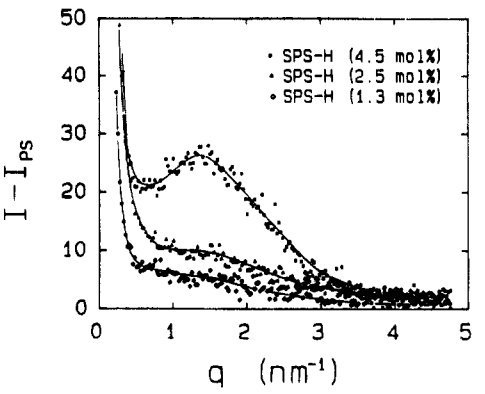

Figure 11. SAXS difference scattering profiles of SPS-H containing, respectively, 4.5 (squares), 2.5 (triangles), and 1.3 mol % (diamonds) of sulfur. The curves were obtained by subtracting the SAXS profile at E = 9432.2 eV and that of polystyrene.

where the intensity contribution from the sulfonic groups has not been removed. This difference becomes more pronounced with decreasing zinc content.

Instead of using zinc, if we measure the SAXS profile of the SPS ionomers in acid form, the much weaker scattering due to the acid sulfonates should reveal similar ionic structures. Indeed, Yarusso and Cooper[5] reported a SAXS peak for the SPS ionomers in acid form at concentrations as low as 1.68 mol %. However, Weiss and Lefelar[29] were able to observe only a shoulder in the SAXS profile for an 11 mol % SPS in acid form and no SAXS peak below 6 mol %. The discrepancy might be attributed to sample preparation. From dynamic mechanical analysis, microphase separation was indicated for SPS acids at $\geq$ 5.8 mol %.[29-31] Thus, we would expect a weak excess SAXS profile for the SPS-H, if it exists. Figure 11 shows SAXS difference profiles of SPS-H containing, respectively, 4.5 (squares), 2.5 (triangles) and 1.3 mol % (diamonds) of sulfur and clearly demonstrates that the sulfonates of SPS ionomers in acid form could aggregate as the neutralized salt form. If sulfonic groups do aggregate, their electron density difference should be relatively small, with an estimated factor of about $10 - 6 = 4$. While in a zinc ion aggregate, the zinc sulfonate has an excess mean atomic scattering factor of $(30 + 10 \times 2)/3 - 6 \approx 11$. Thus, the ratio of the scattered intensity from the zinc sulfonate aggregates to that of the acid sulfonate aggregates is $(11/4)^2 \sim 7$, implying that, if the ionomer aggregates have the same number density as the polymer backbone, a scattered intensity difference of 7 should be observed approximately. We observed a factor of ~6.

V. Conclusions

We have demonstrated that ASAXS can be used to determine the scattered intensity due to ionic aggregates in SPS ionomers. At an appreciable mole percent of sulfonate, SPS-Zn shows a much higher scattered intensity than that of PS in the SAXS region of interest. Consequently, the same excess SAXS profile of zinc sulfonate in SPS-Zn can be determined by using the scattered intensity of polystyrene as the background. ASAXS difference scattering profiles have lower signal-to-noise ratios than the corresponding SAXS difference scattering profiles because ASAXS takes only a fraction of scattered intensity as the unambiguous intensity contribution from the metal ions. Nevertheless, ASAXS could yield a definitive answer as to the origin of the ionic peak and the small-angle upturn; i.e., they are due to the zinc ions. While in a SAXS difference profile with PS as the background,

one can never be certain whether the small-angle upturn could be attributed to voids in SPS-Zn. The essential features of the SAXS profile due to Zn have now been established. We shall select a few SAXS profiles and compare the experimental data with model computations in the next paper.

Acknowledgment. Support of this work by the National Science Foundation, Polymers Program (DMR8921968), and of the SAXS facilities by the Department of Energy is gratefully acknowledged.

References and Notes

(1) See, for examples: Eisenberg, A.; King, M. *Ion Containing Polymers*; Academic: New York, 1977. MacKnight, W. J.; Earnest, T. R., Jr. *J. Polym. Sci., Macromol. Rev.* **1981**, *16*, 41.
(2) MacKnight, W. J.; Taggart, W. P.; Stein, R. S. *J. Polym. Sci., Polym. Symp.* **1974**, *45*, 113.
(3) Roche, E. J.; Stein, R. S.; Russell, T. P.; MacKnight, W. J. *J Polym. Sci., Polym. Phys. Ed.* **1980**, *18*, 1497.
(4) Gierke, T. D.; Munn, G. E.; Wilson, F. C. *J. Polym. Sci., Polym. Phys. Ed.* **1981**, *19*, 1687.
(5) Yarusso, D. J.; Cooper, S. L. *Macromolecules* **1983**, *16*, 1871; *Polymer* **1985**, *26*, 371.
(6) Weiss, R. A.; Lefelar, J. *Polymer* **1986**, *27*, 3.
(7) Fitzgerald, J. J.; Kim, D.; Weiss, R. A. *J. Polym. Sci., Polym. Lett. Ed.* **1986**, *24*, 263.
(8) Gebel, G.; Aldeberg, P.; Pineri, M. *Macromolecules* **1987**, *20*, 1428.
(9) Fujimura, M.; Hashimoto, T.; Kawai, H. *Macromolecules* **1981**, *14*, 1309; **1982**, *15*, 136.
(10) Galambos, A. F.; Stockton, W. B.; Koberstein, J. T.; Sen, A.; Weiss, R. A.; Russell, T. P. *Macromolecules* **1987**, *20*, 3091.
(11) Roche, E. J.; Stein, R. S.; MacKnight, W. J. *J. Polym. Sci., Polym. Phys. Ed.* **1980**, *18*, 1035.
(12) Roche, E. J.; Pineri, M.; Duplessix, R.; Levelut, A. M. *J. Polym. Sci., Polym. Phys. Ed.* **1981**, *19*, 1.
(13) Earnest, T. R.; Higgins, J. S.; MacKnight, W. J. *Macromolecules* **1982**, *15*, 1390.
(14) Clough, S. B.; Cortelek, D.; Nagabhushanam, T.; Salamone, J. C.; Watterson, A. C. *Polym. Eng. Sci.* **1984**, *24*, 385.
(15) Li, C.; Register, R. A.; Cooper, S. L. *Polymer* **1989**, *30*, 1227.
(16) Register, R. A.; Sen, A.; Weiss, R.A.; Copper, S. L. *Macromolecules* **1989**, *22*, 2224.
(17) (a) Ding, Y. S.; Hubbard, S. R.; Hodgson, K. O.; Register, R. A.; Cooper, S. L. *Macromolecules* **1988**, *21*, 1698. (b) Register, R. A.; Cooper, S. L. *Macromolecules* **1990**, *23*, 310.
(18) Register, R. A.; Cooper, S. L. *Macromolecules* **1990**, *23*, 318.
(19) Ding, Y. S.; Register, R. A.; Yang, C.-Z.; Cooper, S. L. *Polymer* **1989**, *30*, 1204, 1213, and 1221.
(20) Register, R. A.; Pruckmayr, G.; Cooper, S. L. *Macromolecules* **1990**, *23*, 3023.
(21) Register, R. A.; Cooper, S. L.; Thiyagarajan, P.; Chakrapani, S.; Jerome, R. *Macromolecules* **1990**, *23*, 2978.
(22) Chu, B.; Wu, D.-Q.; Wu, C. *Rev. Sci. Instrum.* **1987**, *58*, 1158.
(23) Chu, B.; Wu, D.-Q.; Howard, R. *Rev. Sci. Instrum.* **1989**, *60*, 3224.
(24) Chu, B.; Wu, D.-Q.; MacKnight, W. J.; Wu, C.; Phillips, J. C.; LeGrand, A.; Lantman, C. W.; Lundberg, R. D. *Macromolecules* **1988**, *21*, 523.
(25) Wu, D.-Q.; Phillips, J. C.; Lundberg, R. D.; MacKnight, W. J.; Chu, B. *Macromolecules* **1989**, *22*, 992.
(26) Chu, B.; Wu, D.-Q.; Mahler, W. *Mater. Res. Soc. Symp. Proc.* **1990**, *171*, 237.
(27) Phillips, J. C.; Baldwin, K. J.; Lehnert, W. F.; LeGrand, A. D.; Prewitt, C. T. *Nucl. Instrum. Methods Phys. Res.* **1986**, *A246*, 182.
(28) Sasaki, S. *Anomalous Scattering Factors for Synchrotron Radiation Users, Calculated using Cromer and Liberman's Method*; National Laboratory for High Energy Physics, 1984.
(29) Weiss, R. A.; Lefelar, J. A. *Polymer* **1986**, *27*, 3.
(30) Rigdahl, M.; Eisenberg, A. *J. Polym. Sci., Polym. Phys. Ed.* **1981**, *19*, 1641.
(31) Weiss, R. A.; Lefelar, J. A. *Proc. Annu. Tech. Conf. Soc. Plast. Eng.* **1984**, *40*, 468.